https://doi.org/10.5194/egusphere-2025-3029
Preprint. Discussion started: 29 August 2025

Multi-annual and seasonal patterns of Murtèl rock glacier borehole deformation, environmental controls and implications for kinematic monitoring.

Giulio Saibene[1], Isabelle Gärtner-Roer[1], Jan Beutel[2], and Andreas Vieli[1]

[1]Glaciology and Geomorphodynamics Group, Geography Department, University of Zurich, 8057 Zürich, Switzerland
[2]Department of Computer Science, University of Innsbruck, 6020 Innsbruck, Austria

Correspondence: Giulio Saibene (saibene.giulio@gmail.com)

Abstract. Information about rock glacier deformation with depth is crucial for understanding the kinematic processes responsible for variations in rock glacier velocity. The majority of studies on rock glacier kinematics have been limited to surface measurements. Here we present the unique, almost eight-year long record from Murtèl rock glacier of borehole deformation at high temporal resolution. The extracted velocity time series with depth shows that seasonal variations are only observed in the active layer (AL), while in the main ice-rich core and the shear zone deformation rates remain relatively stable. At inter-annual timescales the variability in movement reaches beyond the AL and into the ice-rich core. The AL, ice-rich core and shear zone make up 20%, 24% and 56% of surface displacement respectively. Compared to previous borehole inclinometer data, we find an unusually high fraction of deformation in the AL at Murtèl for the observation period. There are multiple rock glacier studies which report that water input dominates over temperature as a control for the seasonal variations in velocity. In contrast, at Murtèl we find that the years with the highest seasonal peaks in velocity are the years with the warmest summers; while the years with the highest meltwater input have a lower seasonal acceleration in deformation. The borehole deformation and temperature data suggest that the seasonal cycle in AL deformation is strongly related to thermal processes, rather than controlled by water input. Beyond this, three independent approaches for measuring surface displacement were applied and show that the borehole inclinometer and geodetic measurements agree well over a period of almost eight years. The continuous GNSS surface observations slightly overestimate the seasonal acceleration, but match the general background displacement well. Rock glacier velocity has recently been included in the essential climate variable (ECV) of "permafrost". Our borehole deformation data provide novel insight on how representative surface velocities are for rock glacier deformation at depth and on various timescales.

1 Introduction

Rock glaciers are the most prominent permafrost landform found in mountain environments. As they are widely spread, they largely influence the geomorphic evolution of periglacial landscapes, in former times and today. Rock glaciers are bodies of perennially frozen sediment which creep downslope. Active landforms typically creep at rates from a few decimeters to a meter per year (Kellerer-Pirklbauer et al., 2024). Even though measurements of rock glacier movements go back to the early

https://doi.org/10.5194/egusphere-2025-3029
Preprint. Discussion started: 29 August 2025

1900s, only in the last 40 years kinematic investigations have revealed the importance of external forcings on rock glacier creep (Haeberli, 1985; Arenson et al., 2002; Cicoira et al., 2021). Atmospheric warming has been linked to both the irreversible loss of permafrost ice and rock glacier acceleration (Roer et al., 2005; Kääb et al., 2007; Haberkorn et al., 2021; Kellerer-Pirklbauer et al., 2024). Mountain permafrost sites from Svalbard to the Alps have been warming on average 0.41°C per decade (Noetzli et al., 2024). In parallel, periods of pronounced warming rates, such 2015 to 2020 in the Alps, have experienced increasing rock glacier velocity (Kellerer-Pirklbauer et al., 2024). The synchronicity between mean annual air temperatures and rock glacier velocity (RGV) has led to the velocity being added in 2022 as a parameter to the "permafrost" ECV. RGV is defined as the annual average horizontal velocity measured at the surface of a rock glacier (RGIK, 2023). The internal structure of rock glaciers is described to be heterogeneous and, similarly, the vertical velocity profile is not uniform with depth (Haeberli et al., 2006; Emmert and Kneisel, 2017; Buchli et al., 2018; Fey and Krainer, 2020). The surface signal of rock glacier deformation can be typically split into three components: the top coarse-blocky active layer (AL), the main permafrost ice core, and a frozen fine debris-rich layer called the shear zone, where most of the deformation occurs (Arenson et al., 2002; Kenner et al., 2020; Cicoira et al., 2021). The surface movement of a rock glacier is an integrated signal of all these three components. Studies that describe the distribution of deformation across these three layers are scarce and most mountain permafrost sites are limited to measuring deformation at the surface via GNSS stations, photogrammetry or geodetic surveys (Wahrhaftig and Cox, 1959; Barsch and Hell, 1976; Haeberli, 1985; Benedict et al., 1986; Lambiel and Delaloye, 2004; Roer, 2007; Cicoira et al., 2022). Measuring deformation with depth requires the instrumentation of boreholes with inclinometers. The first cases of borehole deformation data are from three rock glaciers in the Engadine limited to annual measurements from 1987 to 1995 (Arenson et al., 2002). This rare deformation data from boreholes showed that, depending on the site, about 60% to over 90% of the surface displacement happens in the shear zone (Arenson et al., 2002). However, the annual temporal resolution did not allow for seasonal investigations of deformation with depth. In 2010, three boreholes were drilled in the destabilized Furggwanghorn rock glacier to measure deformation at higher temporal resolution (Buchli et al., 2018). However, the boreholes survived only up to 10 months because displacements of up to a few meters per years (Buchli et al., 2018). The inclinometer data from Furggwanghorn showed that almost all of the surface displacement occurs at the shear zone and that there seems to be a seasonal pattern (Buchli et al., 2018). Until now it remains unclear whether seasonal fluctuations in surface displacement derive from the shear zone or shallower depths. More borehole sites are needed to evaluate whether the results from Furggwanghorn rock glacier are site-specific or can be applied to other rock glaciers.

At seasonal timescales the controls of rock glacier deformation are still in debate as there are not many studies with high temporal resolution RGV data. Most recent studies report that it is the infiltration of liquid water into the rock glacier core and even down to the shear zone that drives seasonal variations in movement (Ikeda et al., 2008; Wirz et al., 2016; Cicoira et al., 2019b; Kenner et al., 2020; Bast et al., 2024). The other seasonal control of rock glacier creep is the thermal influence. For ice-rich rock glaciers, the plastic deformation component of RGV is considerable. According to the Glen flow law of ice, the temperature of the viscous material is the main driver of its deformation (Nye, 1952). The annual thermal regime of a rock glacier core depends on both the winter and summer atmospheric conditions (Vonder Mühll and Haeberli, 1990; Schneider et al., 2012). So far, it is not trivial to claim whether the summer or winter are more important to establish the

https://doi.org/10.5194/egusphere-2025-3029
Preprint. Discussion started: 29 August 2025

thermal processes driving seasonal variations in deformation. This is because it is unknown from what depths seasonality in creep originates. Often the shear zone is below the depth of zero annual amplitude where temperature cycles have periods greater than a year, so temperature is less likely to drive seasonal variations in shear zone deformation (Buchli et al., 2018). However, if the seasonal deformation cycle were to occur primarily in the shallow subsurface, then summer temperatures would be important. The lack of high resolution borehole deformation data makes it uncertain which processes primarily drive seasonal changes in rock glacier deformation.

The first aim of this study is to use the continuous high temporal resolution deformation record from the 2015 borehole drilled in Murtèl-Corvatsch rock glacier to determine how the integrated components of deformation vary over different timescales and with depth. The second aim of this study is to explore the thermo-hydrological controls of seasonal deformation with depth using the extensive data from Murtèl rock glacier. The last aim is to compare the three approaches available at Murtèl to monitor surface kinematics: borehole inclinometer, GNSS and geodetic survey using a total station.

2 Methods

Murtèl rock glacier, in the Engadine region of the Swiss Alps (Fig. 1) is an active rock glacier located between 2640–2800 m a.s.l. and with a mean annual air temperature (MAAT) of -1.5°C based on the 1998–2022 period (PERMOS, 2024). Murtèl is one of the most investigated rock glaciers worldwide and unique due to its high ice content of approximately 90% ice in the main 20 m thick core (Haeberli et al., 1988; Hoelzle et al., 2002; Gärtner-Roer and Hoelzle, 2021). It is also the slowest moving rock glacier monitored in the Engadine region (Vonder Mühll and Haeberli, 1990; Kellerer-Pirklbauer et al., 2024). The first borehole was drilled in 1987 down to 62 m (COR 1987), which established the first long-term time series of borehole temperatures in the region and also the first deformation measurements from a borehole in a rock glacier (Haeberli et al., 1988; Arenson et al., 2002). The inclinometer installed in 1987 was limited to an annual temporal resolution (Haeberli et al., 1998). In addition, the 1987 drilling allowed for a first description of the stratigraphy of Murtèl rock glacier (Haeberli et al., 1988).

In 2015 a new borehole was drilled a few meters beside the 1987 borehole (COR 2015) to continue the long-term temperature record and install an automatic inclinometer to measure continuous deformation with depth (Fig. 2). The drilling was non-destructive (for more details see Noetzli et al. (2021)), allowing to gather more data about the internal structure of Murtèl rock glacier. The borehole is equipped with thermistor sensors to 60 m depth and an inclinometer chain to a depth of 40 m with sensors every 50 cm. The borehole temperature data is provided directly from the PERMOS data portal (https://www.permos.ch/data-portal). For this study, the borehole temperature is used to calculate the vertical ground heat flux at each sensor's depth using an average thermal conductivity for a rock and ice mixture of 2.5 $Wm^{-1}K^{-1}$ (Vonder Mühll et al., 1998; Scherler et al., 2014). The annual active layer thickness (ALT) is extracted based on the annual maximum depth of the 0°C isotherm found by linearly interpolating between the available thermistors. The periods of phase change in the AL, known as the zero curtains, are extracted by finding the time segments where the temperature from the lowest sensor in the AL remains constant at around 0°C for at least two weeks.

https://doi.org/10.5194/egusphere-2025-3029
Preprint. Discussion started: 29 August 2025

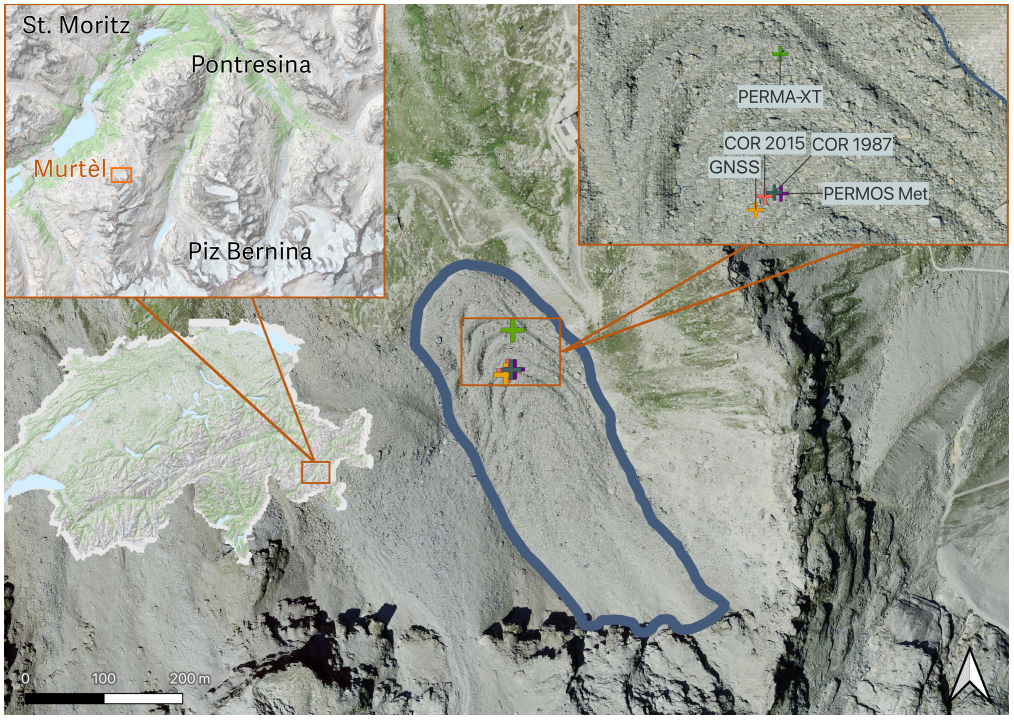

Figure 1. Study site of Murtèl rock glacier (blue outline) with the locations of the two boreholes (COR 1987 and 2015), the GNSS station and the two weather stations (PERMOS and PERMA-XT). Orthophoto derived from SwissTopo (2025).

The borehole deformation data is recorded using a ShapeAccelArray (SAA) field inclinometer made up of 50 cm inextensible segments each measuring tilt angle from the vertical at 8-hour intervals. The measured angles are then converted into *x, y* and *z* displacement using the Measurand software (https://measurand.com/products/data-viewing-and-analysis/).

In 2016, a GNSS station was installed on a large boulder next to the 2015 borehole to measure surface displacement at 30 s intervals and processed at a daily rate. The GNSS also has a two-axis inclinometer that continuously measures the tilt angle. The GNSS instruments are mounted on a mast on top of the boulder, which is around one meter higher than the elevation of the top of the borehole chamber. For specifications about the GNSS station and the data processing procedure refer to Cicoira et al. (2022). Both the SAA and GNSS data are processed by computing *x* and *y* displacement vectors relative to a starting reference position. These displacement vectors are then used to calculate the magnitude of the horizontal deformation at the GNSS station and in each of the segments of the SAA inclinometer with time, resulting in a cumulative daily time series of total horizontal displacement. Differences between daily measurements are then applied to calculate the daily velocity. The velocity data is also aggregated annually based on the calendar year. For the SAA data, layer-specific deformation rates are calculated for the AL, the ice-rich core, and the shear zone by taking the difference of the deformation rates between the top and the bottom values of the given layers. The fraction of deformation that occurs in a given layer relative to the surface displacement is calculated by dividing the layer-specific deformation rate by the total surface displacement over that time. These fractions

https://doi.org/10.5194/egusphere-2025-3029
Preprint. Discussion started: 29 August 2025

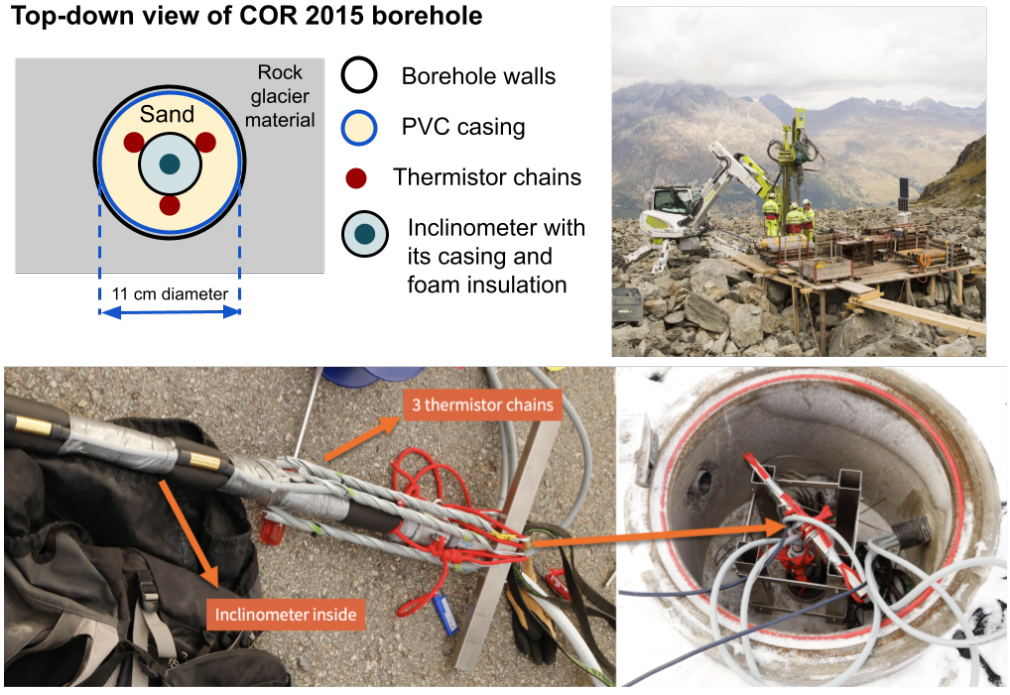

Figure 2. The installation of the 2015 borehole in Murtèl rock glacier. Sketch of the top-down cross-section of the borehole (top-left). Photo of the drilling of the 2015 borehole (top-right). Configuration of thermistor-inclinometer bundle inserted in the borehole with its top concrete chamber (bottom). Photos by Alexander Bast.

are then also calculated from visual inspection of the graphs from the already existing inclinometer deformation profiles of the few older studies to compare the results to other rock glaciers (Arenson et al., 2002; Ikeda et al., 2008). The vertical strain rate is calculated at each depth by differentiating the horizontal deformation rate of each sensor with depth. A vertical profile of annual mean strain rate is used to extract the depth range of the shear zone based on where a peak in strain rate is found. As additional independent displacement observations, being part of the PERMOS monitoring strategy, geodetic surveys are carried out once a year measuring the location of marked boulders around the surface of the rock glacier using a total station (Roer, 2007). Out of the 10 measured points, the one located on the GNSS station boulder, a few meters from the 2015 borehole, is used in this study. The surface displacement is, in total, being measured by three different methods: borehole inclinometer, GNSS and geodetic surveys. These three approaches will be compared and evaluated against each other.

Ten years after the 1987 borehole drilling a meteorological station was installed by PERMOS five meters away from the borehole ((Mittaz et al., 2000)) (Fig. 1). The variables measured that are relevant for this study are air temperature, ground surface temperature, and snow height. For these three variables, the annual means and maxima are computed. The snow height time series is used to calculate: the start of the snow accumulation, the November-January mean snow height, the duration when the snow height is larger than 70 cm (depth at which the thermal regime of the permafrost and that of the atmosphere

https://doi.org/10.5194/egusphere-2025-3029
Preprint. Discussion started: 29 August 2025

become decoupled; Keller 1994; Vonder Mühll et al. 1998; Hoelzle et al. 1999), the April-June mean snow height, the start date of the snow-free period and the daily snowmelt energy. The snowmelt energy is calculated by converting the decrease in snow height into an energy flux using an average snow density of 300 kg/m^3 and a specific latent heat of fusion of water of 334×10^3 J/kg (Scherler et al., 2014). Two temporal phases, *warm* and *cold*, based on seasonal processes are defined using the weather and borehole data. The start of the snow-free period marks the beginning of the warm phase which lasts until the borehole temperature at 0.5 m decreases below 0°C and the cold phase starts. The other *in-situ* climatic station used is the PERMA-XT meteorological station installed in August 2020 which includes an unheated rain gauge to measure rainfall (Amschwand et al., 2023). This rainfall data from 2020 to 2023 is extrapolated back to 1997 based on regression coefficients with the warm phase precipitation data from the MeteoSwiss Piz Corvatsch (located 1.3 km away at 3298 m elevation). The number of dry periods longer than five days per warm phase is then computed using this extended series of rainfall data. The Piz Corvatsch station air temperature measurements are used to fill the data gaps in the air temperature series from the *in situ* PERMOS station using same regression approach as for the rainfall. All listed environmental variables are compared with the deformation data qualitatively and quantitatively using linear regressions. The results of the linear regressions are compiled into a matrix to extract the most significant driving variables for deformation. The combination of the statistically significant variables is then used to train a multiple linear regression model to predict the surface velocity data.

3 Results

3.1 Vertical trends of borehole deformation

The inclinometer installed in Murtèl rock glacier has collected deformation data with depth for nearly eight years (2016–2023; Fig. 3). The uppermost segment of the inclinometer moves at an average of 12 cm/year. Over the total measurement period from August 2016 to July 2023 the top of the borehole moved by a total of 87 cm. Two meters below the surface the average annual deformation rate drops to 9.5 cm/year. This represents a relatively high strain rate in the AL of 0.007 year^{-1} (Table 1). The average strain rate (or vertical gradient of the deformation profile) of the AL is the second highest out of all layers. This high strain rate in the top few meters is visualized in the vertical deformation profile in Figure 3 starting in 2017. The average annual deformation occurring only within the AL is 2.6 cm/year, which makes up about 20% of the surface movement (Table 1). This AL-specific deformation increases with time. The ALT extracted from the borehole temperatures is stable at 3.5 m until 2021 when it deepens to more than 4 m. Below 2 m the strain rate becomes lower, as illustrated by the smaller vertical gradient in the deformation profiles (Fig. 3). A unique feature is observed at around 7–9 m where the deformation reverts to increase with depth before returning to decrease with depth at 9 m (Fig. 3). From 9–21 m the deformation continues to decrease with depth at a relatively constant strain rate. At 21 m the strain rate starts to increase until 26 m, after which the highest strain rates are found in the shear zone. The mean annual deformation in the ice core is 3 cm/year, which is 23% of surface velocity. The shear zone is identified to extend from 26.5–28 m. The velocity decreases there from 6.6 cm/year at 25 m to 0.1 cm/year at 30 m. The shear zone maximum strain rate is 0.04 year^{-1} (Table 1). The annual average deformation rate of the shear zone is 5.9 cm/year or 56% of the surface velocity.

https://doi.org/10.5194/egusphere-2025-3029
Preprint. Discussion started: 29 August 2025

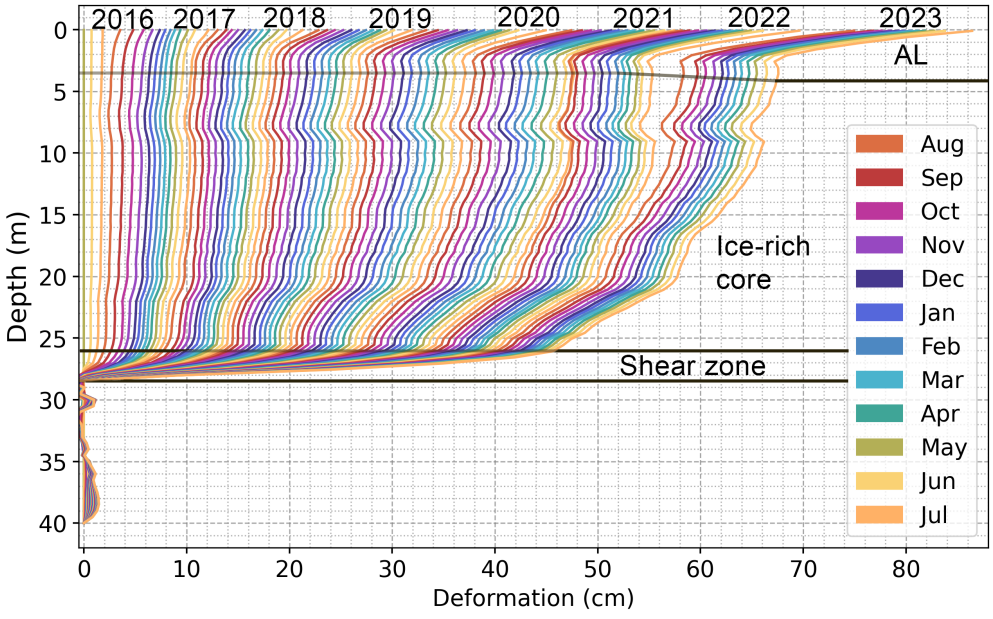

Figure 3. Monthly cumulative deformation profiles from the inclinometer data in the 2015 borehole at Murtèl rock glacier starting in August 2016 and ending in July 2023. The relevant layers of the AL and shear zone are labeled at the according depths.

Table 1. For each of the three layers: the average fraction of the total displacement at the surface, the average deformation rate and strain rate over the entire layer for the 2016–2023 period.

	AL		**Ice-rich core**		**Shear zone**	
Fraction of total displacement at surface (%)	20.2		23.6		56.2	
Layer-specific deformation rate (cm/year)	2.6		3.0		5.9	
Layer-specific strain rate (year^{-1})	0.007		0.001		0.04	
	Top	Bottom	Top	Bottom	Top	Botom
Depth (m)	0	3.5		26.5		28

3.2 Annual trends of borehole deformation

The interannual variability of the borehole deformation varies across different depths. The AL-specific annual deformation rate ranges from approximately 1 cm/year to 6 cm/year (Fig. 4a). The ice-rich core deformation ranges from approximately 1 cm/year to 5 cm/year, and the shear zone deformation stays relatively constant ranging from approximately 6 cm/year to 7 cm/year. A similar pattern of decreasing interannual variability with depth is observed in the annual average borehole temperature profiles (Fig. 4b). During the six years with complete borehole deformation data, the annual deformation rate shows an increasing trend. The years 2020 and 2022 have especially high annual surface velocities at 12.5 and 17 cm/year respectively

https://doi.org/10.5194/egusphere-2025-3029
Preprint. Discussion started: 29 August 2025

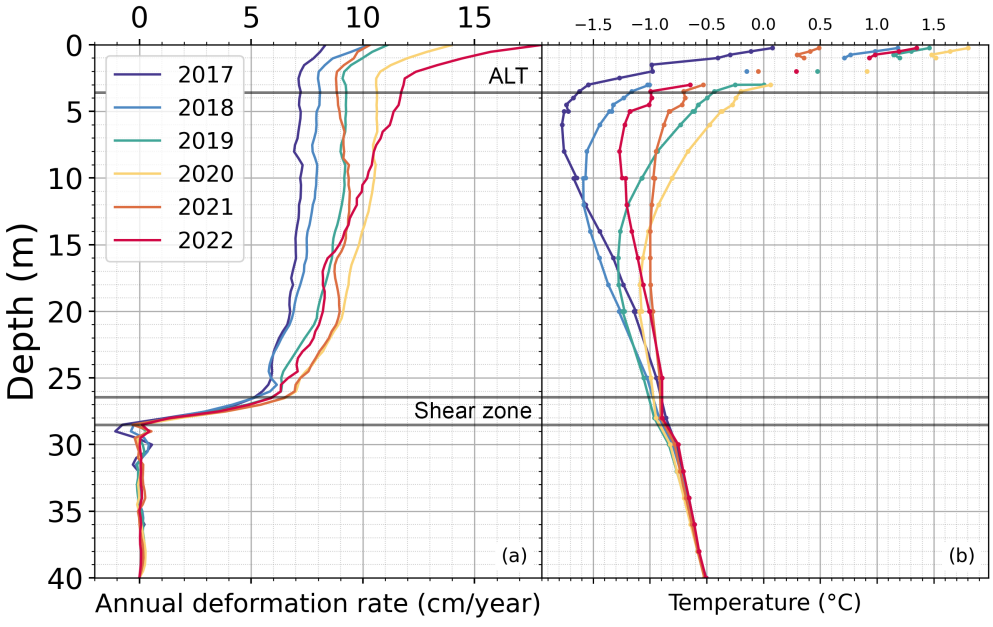

Figure 4. Annual deformation profiles with depth from the borehole with the mean AL-thickness marked as well as the shear zone. **a** Profiles of annual deformation rate from 2016 to 2022. **b** Profiles of annual average borehole temperature from thermistors in borehole. Borehole temperature data from PERMOS (PERMOS, 2024).

(Fig. 5a). The active layer (AL) and ice-rich core deformation are the dominant components to this increase in deformation, whereas the shear zone deformation remains relatively constant. In 2020, the AL contributed to 22% of surface displacement and 37% in 2022. The ice-rich core contributed to 26% of surface displacement in 2020 and 34% in 2022. The AL and ice-rich core deformation accelerate at an average rate of 5.6 mm/year^2 and 3.2 mm/year^2 respectively, while the shear zone deformation decelerates by 1.5 mm/year^2. The annual velocity measured at the surface is not always representative of the deformation at depth. For example, the surface velocity in 2019 was higher than in 2021; however, the opposite is true from 7 m to the shear zone where the velocity is higher in 2021 (Fig. 4a). Similarly, in 2018 the surface velocity was similar to that in 2021; however, the velocity at depth in 2018 is approximately 1.5 cm/year lower than in 2021. From the surface to 8 m the deformation was highest in 2022, while below 8 m the highest deformation was in 2020. However, for some years, such as 2017, when the surface velocity is low, the deformation at depth is also low.

3.3 Seasonal variations of borehole deformation

The daily deformation data measured by the borehole inclinometer allows to investigate the seasonal variations in deformation of Murtèl rock glacier with depth. Of the three identified layers, only the AL consistently experiences a seasonal cycle in velocity with an increase starting in mid-August that peaks around early September followed by lower deformation during the cold phase from November on (Fig. 5b). The deformation rates during the cold phase do not vary much from year to

https://doi.org/10.5194/egusphere-2025-3029
Preprint. Discussion started: 29 August 2025

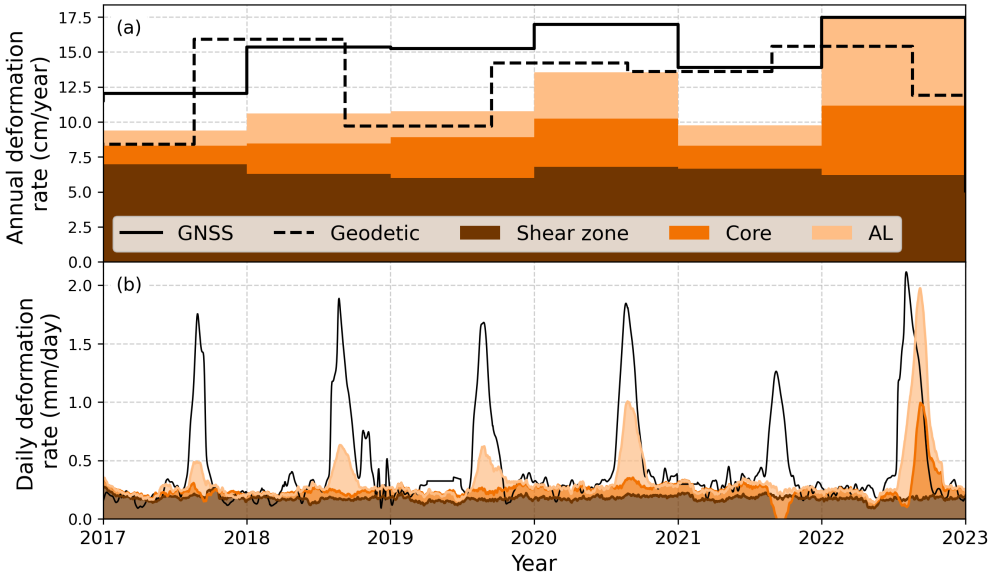

Figure 5. Layer-specific cumulative deformation rates over time: (**a**) at an annual resolution and (**b**) at a daily resolution. Measurement are from the borehole, the GNSS station and the geodetic marker (only with an annual resolution).

year. During the seasonal peaks, the magnitude of the surface velocity is about four times larger than that of the background shear zone rate. In 2020 and 2022, when the seasonal peaks in deformation are especially high, there is also some seasonal acceleration in the ice-rich core deformation as well. In 2022, an increase in daily deformation rate during the warm phase can be seen down to 15 m. In 2021, the seasonal peak in AL deformation is missing and the ice-rich core deformation decreases to negative values; this special event will be discussed in Section 4.3. The shear zone daily deformation rate shows no seasonal pattern and is stable at approximately 0.25 mm/day. Figure 5 also includes the GNSS deformation data at both annual and daily resolutions. Generally, the GNSS station measures similar surface speeds during the winter and similar acceleration patterns in summer as the uppermost sensor in the borehole, but the summer peaks are generally overestimated. The seasonal peaks in deformation rate of the GNSS are 67% higher than those measured at the top of the borehole inclinometer, but generally align well in terms of timing. The only year when this is not the case is 2022 when the GNSS peak occurs one month before the inclinometer peak. The annual displacements measured by the geodetic surveys in late August generally follow the annual fluctuations from the borehole deformation with an increase in deformation in 2018, 2020 and 2022 (Fig. 5a). There are large differences in annual deformation between the geodetic measurements and the inclinometer from 2017–18 and 2021–22 (see Section 4.4).

3.4 Seasonality in atmospheric conditions and borehole temperatures

The strong seasonality in both the atmospheric conditions and borehole temperatures is illustrated in Figure 6a. The annual snowfall amount is rather variable, with winters such as 2021–22 and 2022–23 having low snow accumulation, while others

https://doi.org/10.5194/egusphere-2025-3029
Preprint. Discussion started: 29 August 2025

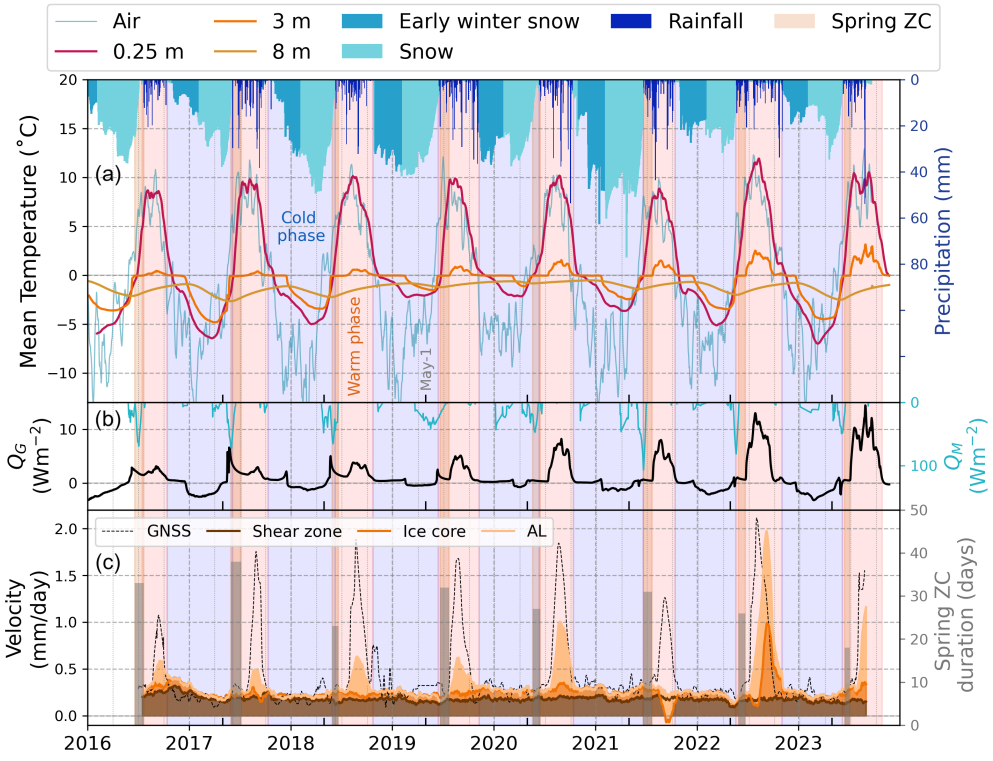

Figure 6. Temporal variations in deformation in context of external climatic forcings. (**a**) Daily snow height, daily precipitation rate and air temperature for Murtèl together with borehole temperatures at 0.25 m, 3 m and 8 m from the 2015 borehole (data from PERMOS; PERMOS 2024). (**b**) Ground heat flux (Q_G) measured at 3.5 m in the 2015 borehole and snowmelt energy flux (Q_M). (**c**) Daily layer-specific deformation rate for AL, ice-rich core and shear zone together with the GNSS daily deformation rate and the spring zero curtain (ZC) duration. The spring ZC is shaded in light orange, the warm phase is shaded in a lighter orange and the cold phase is light blue.

such as 2020–21 having high snow accumulation. The air temperature and the temperature at 0.25 m depth in the borehole closely follow each other during the warm phase, while in the cold phase the air temperature is clearly colder than the temperature at 0.25 m depth. The maximum warm phase temperature at 0.25 m is relatively constant at about 10°C, except for the colder summers of 2016 and 2021, and the warm summer of 2022. The minimum cold phase temperature at 0.25 m is more variable from approximately -6°C to -2°C. The duration of the warm phase ranges from 110 to 165 days, with 2021 having the shortest warm phase and 2022 the longest. The duration of the cold phase ranges from 210 to 250 days, with 2020 having the shortest cold phase and 2021 the longest (Appendix Table A1). The snowmelt energy peaks from late May to early June occur soon before the start of the spring zero curtain in the AL. On average, the spring zero curtain lasts about one month from May to June and the snow melts out by June 15. The AL starts to freeze on October 19 and the autumn zero curtain typically starts in October and ends in November (Appendix Table A2). The annual maximum ground heat flux at 3.5 m occurs during snowmelt for the first three years, and after 2019 it occurs later in the summer before the maximum AL temperatures are reached. The

https://doi.org/10.5194/egusphere-2025-3029
Preprint. Discussion started: 29 August 2025

interaction of such seasonality and the thermo-hydrological processes relevant for rock glacier deformation are discussed in Section 4.2.

4 Discussion

4.1 Layer-specific contributions to deformation

The active layer (AL) is the only layer in Murtèl rock glacier to experience a consistent seasonal cycle in deformation. When compared to other rock glaciers with shorter and older data series, Murtèl has a high fraction (20%) of surface displacement happening in the AL (Table 2). Findings from the few other sites report at most 8% of surface displacement occurring in the AL (Table 2). The AL of Büz North rock glacier is one of lowest deforming AL and is composed of finer sediment compared to the especially coarse AL of Murtèl rock glacier. So, this would suggest that coarser ALs experience more deformation. However, Arenson et al. (2002) state that there is a larger increase in shear resistance caused by the interlocking forces of the individual coarse blocks compared to smaller ones. More quantitative investigations are needed to better evaluate the effect of grain size distribution on AL deformation. The higher vertical strain rate in the AL compared to the ice-rich core from the deformation profiles presented here is consistent with earlier observations from the 1987 borehole at Murtèl (Appendix Fig. C1; Arenson et al. 2002). A similar secondary shear zone feature in the AL is also seen in a shallow inclinometer at Ritigraben rock glacier (Lugon and Stoffel, 2010). However, in most of the other rock glacier inclinometer measurements, this is not observed (Arenson et al., 2002; Buchli et al., 2018). The large variation in the contribution of the AL to surface displacement is likely due to the roughness of the permafrost table, the differences in the grain size of the AL, or the local microtopography around the borehole.

The 23 m thick ice-rich core in Murtèl rock glacier makes up 26% of the total surface displacement. The inclinometer measurements from the 1987 borehole at Murtèl report that the ice-rich core contributes to about 33% of surface movement (Arenson et al., 2002). Muragl and Schafberg rock glaciers have an ice core contribution to surface displacement of 3–47% and 17–20% respectively (Table 2). Furggwanghorn rock glacier has close to zero ice core deformation (Buchli et al., 2018), hence, there is a large variation in the ice core contribution to rock glacier deformation between rock glaciers. The creep behavior of debris-poor ice is known to depend on the ice content and grain size, which affect the strain rate response to the applied shear stress (Cicoira et al., 2021). Various laboratory experiments found that when the debris content exceeds about 40%, the interlocking forces between debris particles become dominant, increasing the shear resistance and thus reducing the strain rate (Bucki and Echelmeyer, 2004; Ladanyi, 2003; Moore, 2014). So, rock glacier ice cores with low debris content should experience higher strain rates and therefore a larger contribution to surface displacement. The other control of plastic deformation in an ice-rich core is its temperature. Glen's law for ice flow states that stress and temperature are mainly influencing creep, and for rock glaciers this is relevant when the debris content is lower than 40%, such as in the case of the Murtèl ice-rich core (Moore, 2014). In fact, the annual deformation rate of the ice-rich core at Murtèl rock glacier is on average accelerating by 3.2 mm/year^2 in parallel to the ice-rich core warming by 0.03°C/year. The deformation in the ice-rich core experiences seasonal fluctuations only during years with very large seasonal peaks at the surface, for example, in 2020 and 2022. The cause

https://doi.org/10.5194/egusphere-2025-3029
Preprint. Discussion started: 29 August 2025

of seasonal peaks in ice-rich core deformation is unclear, but it is likely related to thermal or hydrological processes. In 2020 the annual mean ice-rich core temperature was the warmest of the 2016 to 2023 period, and the annual deformation in the ice-rich core was clearly enhanced (Fig. 5). The thermal processes related to deformation will be discussed in Section 4.2.2. The relatively large proportions of AL and ice-rich core deformation mean that, for Murtèl, the surface velocity is 5.4 cm/year higher than the velocity at the top of the shear zone.

Table 2. Layer-specific fractions of surface displacement calculated from deformation profiles in different rock glacier boreholes instrumented with an inclinometer. Values in parenthesis are from Arenson et al. (2002) if different from ones reported here.

Borehole	AL (%)	Ice core (%)	Shear zone (%)	Shear zone depth (m)
Murtèl 2015	20.2	23.6	56.2	26.5–28
Murtèl 1987[a]	8	33	59	28–31
Schafberg 1/1990[a]	5	3	92 (97)	11–16
Schafberg 2/1990[a]	1	47	52 (50)	24–26
Muragl 3/1999[a]	3	20	77	16–18
Muragl 4/1999[a]	8	17	75 (82)	14–16
Büz North[b]	0.7–2	–	–	–

[a] Arenson et al. (2002)
[b] Ikeda et al. (2008)

The largest fraction of surface displacement at Murtèl occurs in the shear zone between 26.5–28 m. The 1987 inclinometer data measured a deeper shear zone at 28–31 m (Arenson et al., 2002). The depth of the shear zone between the two boreholes is difficult to compare as the two boreholes are in different locations and the shear zone plane is likely not flat. The fraction of deformation happening in the shear zone in the 2015 borehole agrees relatively well with that of the old 1987 inclinometer. At other rock glaciers with inclinometers down to the shear zone, the fraction to total deformation varies greatly (Table 2). Murtèl rock glacier is the one with the lowest shear zone contribution to surface displacement across the three rock glaciers in Table 2. Furggwanghorn rock glacier has shear zone displacement that is almost equal to its surface displacement (Buchli et al., 2018). The fraction of surface displacement that occurs in the shear zone may depend on the stratigraphy of the shear zone, the depth where it is found, and its temperature regime. At Murtèl, the ice content above the shear zone is still high with only some thin layers of fine sediment. In the shear zone the ice content decreases and it is composed of frozen fine sediment with a few coarser particles. Below the shear zone the debris becomes coarser and the ice content drops to close to zero. This high anisotropy in the stratigraphy around the shear zone leads to strain localization, increasing the shear zone deformation contribution (Moore, 2014). The shear zones found at shallower depths measure high contributions to surface displacement compared to the deeper shear zones (Table 2). At Murtèl rock glacier the shear zone is found below the depth of zero annual amplitude, so at a seasonal timescale it experiences negligible temperature fluctuations. The shallower shear zones are more likely to be above the depth of zero annual amplitude, and hence experience larger temperature variations and more

https://doi.org/10.5194/egusphere-2025-3029
Preprint. Discussion started: 29 August 2025

deformation. In summary, compared to other sites, Murtèl rock glacier has a relatively low fraction of total deformation in the shear zone and relatively high deformation in the ice-rich core and the AL.

4.2 Seasonal controls of deformation

4.2.1 Cold phase controls

During the cold phase, the snowpack acts as an insulator to the permafrost temperatures below and this has consequences on the deformation. Figure 6a shows how, during the cold phase, the decrease in temperature in the borehole is more attenuated compared to the decrease in air temperature. An early winter with high snow accumulation leads to milder permafrost temperatures (Hoelzle et al., 1999; Kenner et al., 2020; Amschwand et al., 2023). The amount of snow accumulation from November to January has a positive and significant correlation with the average temperature from March to April at the top of the permafrost table for the periods 1997–2022 and 2016–2022 ($R^2 = 0.64, 0.79$ respectively). The years with the most negative ground heat flux during the cold phase are also the years with least snow accumulation during the early winter (Fig. 6a–b). So, a persistent thick snow cover is associated with a reduction in winter cooling of the permafrost at depth. Beneath the AL the warm phase temperatures depend on the cold phase temperatures. In fact, a linear regression analysis between the cold and warm phase temperatures at given depths found significant correlations only below the AL (Appendix Fig. B2). The duration of a deep snowpack (i.e. > 70 cm) is moderately correlated with the warm phase mean ice-rich core temperature for the two boreholes ($R^2 = 0.45, 0.49$ respectively). Therefore, as early winter snow accumulation affects the cold phase temperatures in the ice core, it also indirectly controls the temperature of the following warm phase. The warm phase temperature is strongly correlated with the annual deformation within the ice core (Appendix Fig. B1c). So, years with a snow-rich early winter experience more mild winter borehole temperatures, which at depths from around 8 m are followed by also milder warm phase temperatures and thereby higher deformation.

4.2.2 Warm phase controls

At Murtèl rock glacier the snowmelt peaks towards the end of May after which the spring zero curtain (ZC) measured in the active layer (AL) begins and lasts until the end of June to the middle of July (Fig. 6). Many rock glacier kinematic studies report seasonal surface acceleration during or shortly after the spring melt (Ikeda et al., 2008; Kenner et al., 2020; Bast et al., 2024). The relatively high water flow speed measured in rock glaciers indicates a high drainage efficiency of meltwater, with a short response time of high pore water pressures (Krainer and Mostler, 2002; Buchli et al., 2013; Bast et al., 2024). However, on Murtèl, it takes two to three weeks from seasonal melt to the start of acceleration in displacement, compared to only a few days for eight other rock glaciers (Buchli et al., 2013; Wirz et al., 2016; Kenner et al., 2020). Moreover, Murtèl takes an average of approximately 50 days from the end of the spring zero curtain to when the maximum surface velocity occurs (Appendix Table B1). Direct measurements of water content in Murtèl rock glacier are not available, therefore the timing and duration of the snowmelt and spring zero curtain are used as proxies for meltwater production. Years with a later snowmelt peak experience lower surface displacement. The mean snow height in April to June is not found to be correlated with the total

https://doi.org/10.5194/egusphere-2025-3029
Preprint. Discussion started: 29 August 2025

deformation measured by the inclinometer over the years ($R^2 = 0.1$) and is negatively correlated with the maximum GNSS velocity ($R^2 = 0.6$). This suggests that years with more snow to melt in spring have a lower peak in surface velocity. In 2021 after a snow-rich winter and a mild and wet summer, Murtèl rock glacier had its lowest seasonal peak in deformation rate, while the nearby Schafberg rock glacier had its highest annual deformation. So, different rock glaciers can react differently to a given hydrological forcing (Bast et al., 2024). For three rock glaciers in the Matter Valley, Switzerland, short peaks in surface velocity were measured shortly after rainfall rates of 10 mm/day or above (Wirz et al., 2016). However, at Murtèl rock glacier no large precipitation events were observed before the seasonal peaks in surface velocity. At Dirru rock glacier, Cicoira et al. (2019b) report that seasonal acceleration is driven by the water input from snowmelt and rainfall. The sum of warm phase precipitation at Murtèl does not have significant correlation with the magnitude of peak surface velocity. Further, the summers with the highest deformation rates typically had the highest number of dry periods longer than 5 consecutive days. So, at a seasonal timescale, the drier summers at Murtèl experienced larger deformation. (Amschwand et al., 2023) found that at Murtèl dry AL conditions do not allow turbulent fluxes to export as much of the incoming energy from solar radiation. As a result, a higher ground heat flux into the AL is experienced, which as discussed below, is found to be an important driver for the magnitude of seasonal acceleration. All of this points to hydrological processes not being the main driver for the timing and magnitude of the seasonal acceleration of Murtèl rock glacier.

Thermal processes in the active layer (AL) during the warm phase are important for acceleration in the AL displacement. The timing of the end of the spring zero curtain sets the start of the snow-free period and of positive ground heat flux through the AL during the warm phase. The earlier the spring zero curtain ends, the warmer the AL becomes, as the coupling between the atmosphere and the AL begins earlier (Fig. 7a). Similarly, an early end to the spring zero curtain is often followed by the AL reaching its annual maximum thickness earlier (Fig. 7b). Figure 7c–d show how the annual maximum GNSS velocity is highest when the melt period happens earlier in the season. The GNSS velocity is highest when the AL rapidly reaches its maximum temperature (Figure 7f–d). So, there is important statistical evidence at Murtèl linking the AL thermal regime and the surface displacement. However, the process behind this is unclear as during the summer the AL should be mostly ice-free. During the drilling of the borehole in summer of 2015 ice was found within the AL starting from 2.7 m. Amschwand et al. (2024) suggest that at Murtèl 20–30% of the snowmelt can refreeze in the coarse pores near the bottom of the AL. This refrozen ice near the bottom of the AL may be the responsible agent linking the thermal regime of the AL to its deformation. Four thermal variables: air and surface temperature, ground heat flux at the top of the permafrost table, and AL mean temperature are sufficient to build a statistically significant multiple linear regression model to predict the monthly GNSS velocity ($R^2 = 0.66$, Appendix Fig B3). The most statistically relevant variable for this model was the ground heat flux into the permafrost table. The ground heat flux experiences positive peaks only down to the permafrost table, while below the high ice content prevents large changes in temperature. Amschwand et al. (2023) found that the AL of Murtèl absorbs 70% of the incoming energy. The ground heat near the bottom of the AL may be warming the refrozen ice and increasing its deformation. The uppermost deformation measurements from the inclinometer are found to be statistically less well correlated with the variables that describe the thermal state of the AL. Only the AL thickness has a significant positive correlation with the SAA displacement at the surface and at

https://doi.org/10.5194/egusphere-2025-3029
Preprint. Discussion started: 29 August 2025

3.5 m (p-value = 0.004 and 0.002, respectively). The differences between the surface velocity measured by the GNSS and inclinometer are explored in Section 4.4.

On average, the time lag between the annual maximum air temperature and GNSS velocity is only 15 days. At Ritigraben, Muragl and Schafberg rock glaciers the time lag between the annual peak in ground surface temperature and surface velocity is much longer at 2–3 months (Cicoira et al., 2019a). The shorter time lag between temperature and velocity at Murtèl exemplifies the important link between temperature and creep at Murtèl for a seasonal timescale. The maximum temperature at 10 m occurs 5 months later than at the surface, which is similar to the 6 months observed by Vonder Mühll and Haeberli (1990). So, only at longer timescales the temperature at depth can be a general indicator of the deformation at depth. In Figure 4b the cold temperature profiles for 2017 and 2018 agree well with the lower annual deformation rate for these years. Similarly, the warm temperature profile for 2020 corresponds to a high annual deformation rate. Note that in 2022 the temperatures in the ice core are not particularly high; however, the ice core deformation in 2022 was the highest of this period. This exception to the coupling between temperature and deformation is discussed in Section 4.3. The correlation between the mean annual temperature and the annual deformation is the strongest for depths from 8–15 m (Appendix Fig. B1a). Overall, the data from Murtèl rock glacier leans toward thermal processes being more critical for the seasonal cycle in AL displacement compared to the hydrological ones. More direct measurements of pore water pressure near the permafrost table would be needed to further test this claim. In 2022 both Murtèl and Schafberg recorded one of the highest AL summer temperatures; however, Murtèl experienced its highest seasonal deformation peak, while Schafberg one of its lowest (Bast et al., 2024). This highlights how different rock glaciers respond differently to seasonal external forces. It is important to consider that due to the variety of internal structures found across different rock glaciers there may not be a universal dominant seasonal control of deformation.

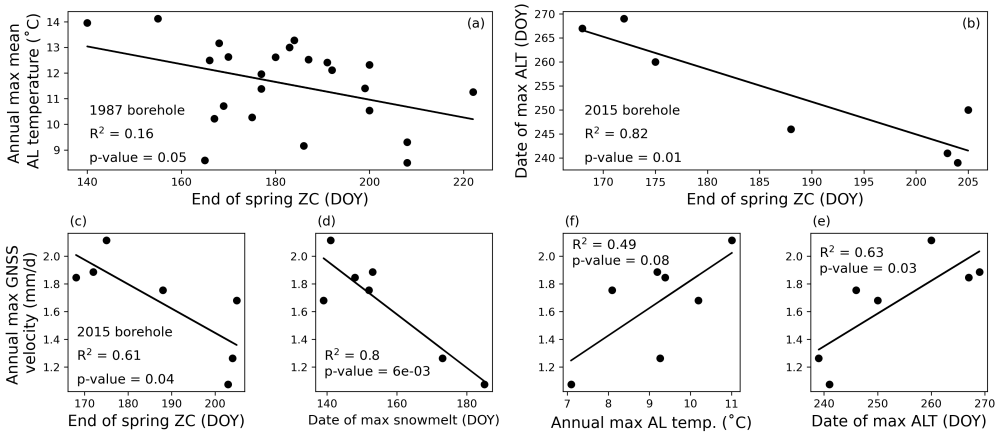

Figure 7. Linear regression analysis between the end of spring zero curtain (ZC) and the annual maximum mean AL temperature for (**a**) the 1987 borehole data and (**b**) the 2015 borehole data. Linear regression analysis for years 2016–2022 between the annual maximum GNSS velocity and (**c**) the date of the end of the spring ZC, (**d**) date when snowmelt is the highest, (**e**) the annual maximum AL temperature, and (**f**) the date when AL thickness reaches its maximum. Data source: PERMOS (PERMOS, 2024).

https://doi.org/10.5194/egusphere-2025-3029
Preprint. Discussion started: 29 August 2025

4.3 Inclinometer behavior and unusual deformation profiles

In the daily time series of borehole velocity data there are two summers that stand out: that of 2021 and 2022 (Fig. 5). From August to September 2021 the AL and ice core velocity decrease and in the ice core negative velocities are measured. In the vertical deformation profile of 2021 the most pronounced inversion in velocity is observed at the top of the ice core and extends down to only about 5 m (Appendix Fig. C2). Below approximately 15 m the deformation remains positive and relatively constant. It is difficult to say what caused the apparent backward movement of the inclinometer segments at the top of the ice core, however, it can be speculated that some blocks towards the bottom of the AL became temporarily locked with each other while the lower ice core kept creeping, causing a backward bend in the rigid casing of the borehole. Another alternative is that the inclinometer chain itself buckled backward within the casing due to the filling material moving. The GNSS station measured the lowest surface velocity peak during 2021. So, the fact that the GNSS did measure a seasonal velocity peak while the inclinometer did not supports the idea that the cause of this inclinometer behavior is structural and specific to the borehole location. The lack of a velocity peak in 2021 is also what caused the correlation analysis to be weaker with the inclinometer data compared to the GNSS data. In 2022 an almost opposite inclinometer behavior occurs, where towards the bottom of the AL a strong acceleration in August and September occurs after a deceleration around the middle of May (Appendix Fig. C3). The transition from deceleration to acceleration would suggest a stick-slip event of blocks in the AL. However, as this is the only year when a seasonal acceleration signal can be measured down to 15 m, it is unclear whether this event originated at the permafrost table or deeper in the ice core. Both 2021 and 2022 had the largest deviations in terms of horizontal direction of movement, which would support the idea of a structural blockage causing a change in the flow direction (Appendix Fig. C4). It may also be important to consider that the warm phase of 2022 was the hottest and longest since 2016. Further observations of similar inclinometer behavior from other sites are needed to better evaluate the responsible processes of such events.

4.4 Evaluating the methods to measure surface displacement

The GNSS station at Murtèl rock glacier measures more deformation than the borehole inclinometer, although the two stations are only a few meters apart. The net total displacement of the GNSS station calculated from the distance of its position in July 2016 to August 2023 is of 101 cm while aggregating the displacement of the uppermost borehole inclinometer yields 87 cm. The daily GNSS displacement rates combined result in a total of 112 cm (Fig. 8). Here, integrating the daily displacements of course aggregates individual daily positioning errors and possibly amplifies filtering applied to the raw data. In fact, integrating the less noisy monthly displacements results in a lower total displacement of 102 cm which is closer to the net total displacement of 101 cm. Most of the discrepancy between the GNSS and inclinometer data occurs during the warm phase when the seasonal peaks in GNSS deformation surpass those of the SAA (Fig. 5). The GNSS station is mounted on a tall boulder that might exhibit additional rotational movement on top of the translational movement, leading to higher measurements of perceived deformation. In fact, the inclinometer of the GNSS station measures an increase in tilt during the seasonal acceleration in surface displacement (Appendix Fig. C5). Moreover, the geodetic marker used to measure deformation with the total station is located on the same boulder as the GNSS station, so differences in total deformation must to some degree be due to the

https://doi.org/10.5194/egusphere-2025-3029
Preprint. Discussion started: 29 August 2025

tilting effect of the 1.0 m mast on top of the boulder where the GNSS antenna is mounted. Future studies using GNSS data to monitor the surface kinematics of rock glaciers should correct for rotational movement as well as non horizontal antenna positions, e.g. based on the approach outlined by Wirz et al. (2014). It should be noted that although the GNSS velocity peaks are approximately 67% larger than the SAA velocity peaks, the difference is only a few millimeters per day. This suggests that likely the peak magnitudes are sensitive to the noise filtering function used (Cicoira et al., 2022). If the monthly GNSS velocity data, which requires less noise filtering, is used instead of the daily then the peaks are smaller. The timing of the seasonal velocity peaks is very similar between the GNSS and borehole inclinometer data (Fig. 5b).

The geodetic deformation measured annually over the entire period differs only by 2 cm relative to the total deformation measured by the SAA inclinometer (Fig. 8). At first sight this is perhaps surprising given the large difference between the annual geodetic deformation rates and those of the SAA in Figure 5. It is, however, important to note that the annual geodetic survey dates are at the end of August, such that in most years the seasonal deformation peak is not fully captured. A sensitivity analysis using alternative survey dates to calculate annual deformation rates from the GNSS and SAA data reveals that surveying at the end of September is sufficient to capture the appropriate annual acceleration signal, even if the average end of the seasonal surface velocity peak happens on October 20. So, future geodetic surveys on Murtèl rock glacier are recommended to take place around the end of September or later given that early winter snow cover is absent. In summary, at high temporal resolution, the GNSS measures higher deformation peaks compared to the borehole inclinometer, although their timing agrees well. Over multiple years, the GNSS shows higher displacements than both the inclinometer and geodetic measurements, while the inclinometer and geodetic measurements are similar.

https://doi.org/10.5194/egusphere-2025-3029
Preprint. Discussion started: 29 August 2025

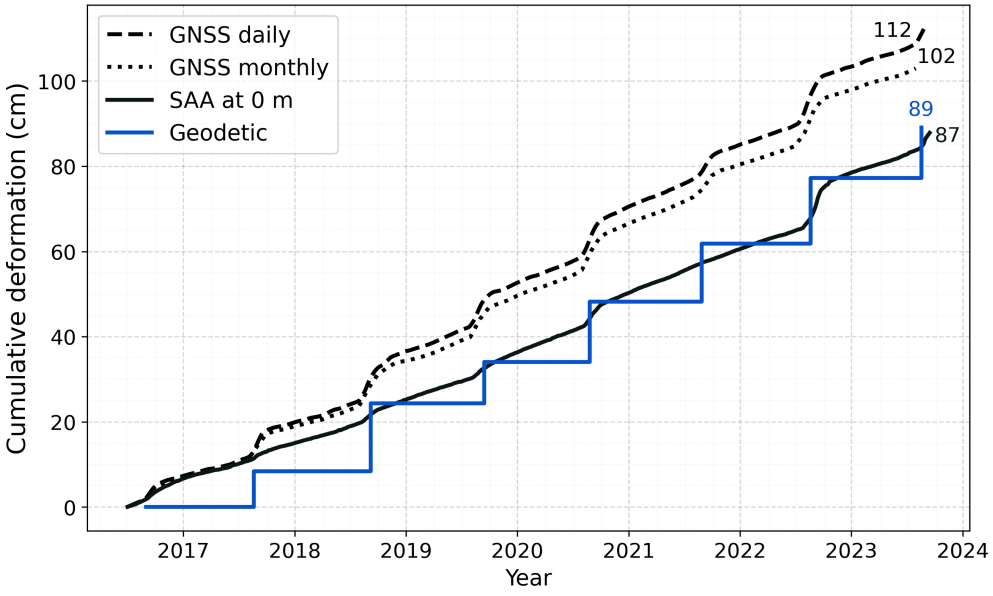

Figure 8. The cumulative displacement measured by the GNSS station, the SAA over the entire depth, and the geodetic station. The GNSS and SAA are available are daily resolution from July 2016 to August 2023, while the geodetic data is limited to an annual resolution. The monthly GNSS data is also shown for comparison. The total displacement (cm) measured over the entire observation period by each technique is also noted. Note the divergence of the GNSS from the inclinometer data is due to the higher displacement during the summer periods. Data source: PERMOS and PermaSense.

5 Conclusions

At Murtèl rock glacier temperature and deformation are both continuously measured in a borehole since 2016. These observations are complemented with a GNSS station, annual geodetic surveys and a meteorological station. This provides a unique dataset and opportunity to investigate rock glacier kinematics in detail including deformation with depth. The borehole deformation data collected for nearly eight years indicate that, on an interannual timescale, most of the temporal variation in deformation is driven by the active layer (AL) and the ice core. On a seasonal timescale, fluctuations are evident only in the AL, and at lower magnitude and only for a few single years in the ice core. The shear zone deformation remains constant at around 5.9 cm/year throughout the observation period. Compared to the few other rock glaciers with borehole deformation data, we observe a larger proportion of deformation occurring in the AL. In terms of the thermo-hydrological processes relevant for deformation, the thermal forcing seem to dominate over the hydrological processes for explaining the summer acceleration in deformation at Murtèl rock glacier. The years with the warmest summers had the highest deformation, but the years with highest snowmelt water input did not experience particularly high deformation. Past rock glacier studies found opposing results with water controls dominating temperature controls. Compared to other rock glaciers, Murtèl has a high ice content and cold temperatures, suggesting that processes driving kinematics at Murtèl are, to some extent, site-specific. Over the entire almost 8

https://doi.org/10.5194/egusphere-2025-3029
Preprint. Discussion started: 29 August 2025

year measurement period, the geodetic measurements of surface displacement match very well with the total deformation from the inclinometer (only a 2% difference). At an annual timescale there are larger differences in the measured deformation rates between the inclinometer and the geodetic station, which can largely be explained by the different timing of the measurements. The continuous GNSS data agrees well with the winter background velocity and the timing of the summer acceleration pattern as measured by the inclinometer. However, the magnitude of the GNSS velocity peaks are higher than those inferred from the inclinometer measurements. The finding that most of the seasonal acceleration is limited to the active layer raises the question whether, on a longer term, trends in rock glacier velocity can be used to describe an ECV. For this, it is important to continue the long-term monitoring of rock glacier deformation, especially with depth. This study shows how the unique seven-year record of high resolution deformation and temperature data with depth combined with meteorological data is invaluable to identify subsurface processes and related forcings. Although Murtèl is considered a special rock glacier, some of the findings and related processes are relevant and transferable to other sites where long-term borehole data is not available.

Data availability. The PERMOS borehole temperature and weather data is all available through their online data portal at https://www.permos.ch/data-portal. The precipitation data used from the PERMA-XT station is available at https://www.permos.ch/doi/permos-spec-2023-1. The Piz Corvatsch weather station data is available upon request from MeteoSwiss. The deformation data will be made available at a later stage of the publication process.

Appendix A: Phases and zero curtains

Table A1. Durations in days of the cold and warm phase for each hydrological year.

Hydrological year	Cold phase duration (days)	Warm phase duration (days)
2016	238	143
2017	225	147
2018	223	145
2019	218	120
2020	253	113
2021	219	171
2022	211	–

https://doi.org/10.5194/egusphere-2025-3029
Preprint. Discussion started: 29 August 2025

Table A2. The spring and autumn ZC duration, start and end dates for each year based on the 2015 borehole temperatures.

Year	Spring ZC (days)	Spring Start	Spring End	Autumn ZC (days)	Autumn Start	Autumn End
2016	33	06-18	07-21	28	10-24	11-21
2017	38	05-30	07-07	26	10-15	11-10
2018	23	05-29	06-21	29	11-03	12-02
2019	32	06-22	07-24	98	11-23	02-29
2020	27	06-20	07-16	42	10-28	12-09
2021	31	06-22	07-23	38	11-07	12-15
2022	26	06-22	06-24	–	–	–
2023	18	06-16	07-04	46	11-15	12-31

Appendix B: Controls on deformation

https://doi.org/10.5194/egusphere-2025-3029
Preprint. Discussion started: 29 August 2025

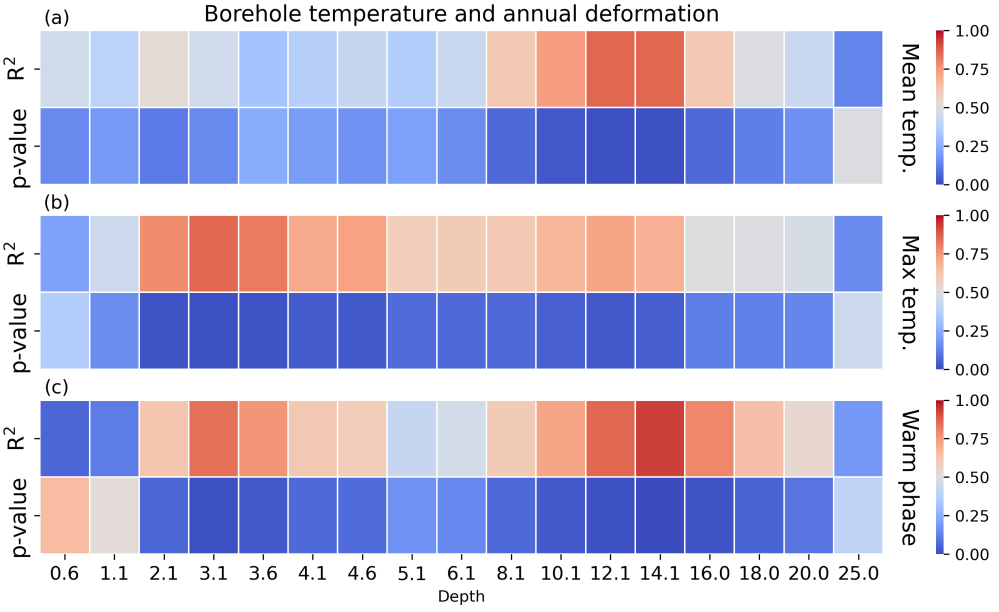

Figure B1. Linear correlation matrix showing the R^2 and p-value of regressions between the mean (**a**), maximum (**b**) and warm phase (**c**) annual borehole temperature at various depths and the annual deformation at that depth.

https://doi.org/10.5194/egusphere-2025-3029
Preprint. Discussion started: 29 August 2025

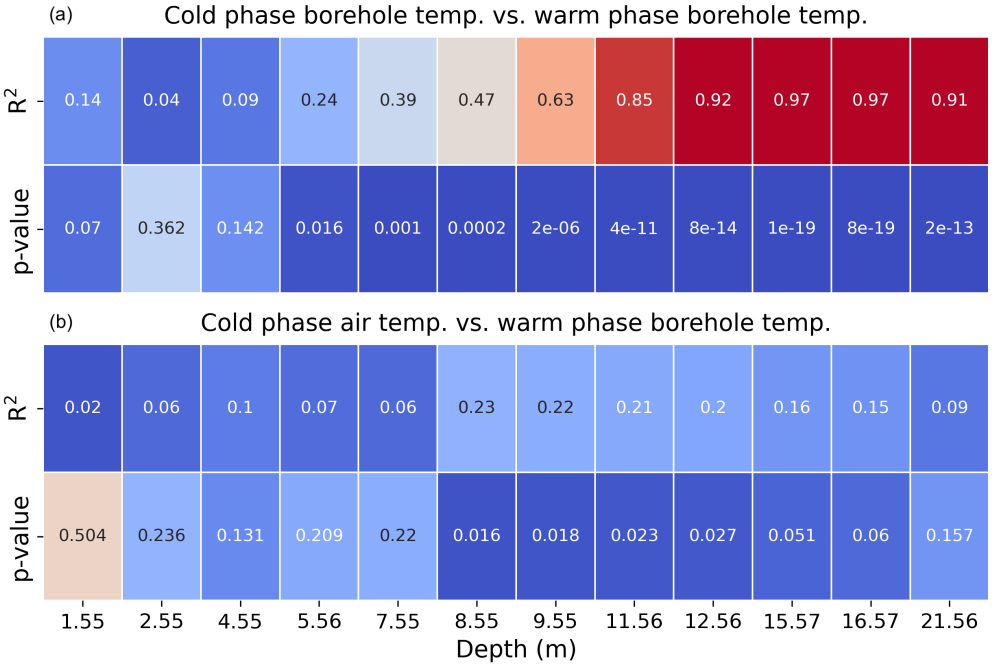

Figure B2. Linear correlation matrix showing the R^2 and p-values of regressions between the mean cold phase borehole temperature and the mean warm phase borehole temperature at varying depths (**a**); and between the mean cold phase air temperature and the mean warm phase borehole temperature at varying depths (**b**) from 1998 to 2022.

https://doi.org/10.5194/egusphere-2025-3029
Preprint. Discussion started: 29 August 2025

Table B1. Yearly data of spring ZC end dates based on the 2015 borehole temperatures, date of maximum GNSS surface displacement, and the time lag between the two.

Year	End date of spring ZC	Date of max GNSS displacement	Time lag (days)
2016	07-21	09-12	53
2017	07-07	08-28	52
2018	06-21	08-23	63
2019	07-24	08-26	33
2020	06-16	08-21	66
2021	07-23	09-07	46
2022	06-24	08-03	40

https://doi.org/10.5194/egusphere-2025-3029
Preprint. Discussion started: 29 August 2025

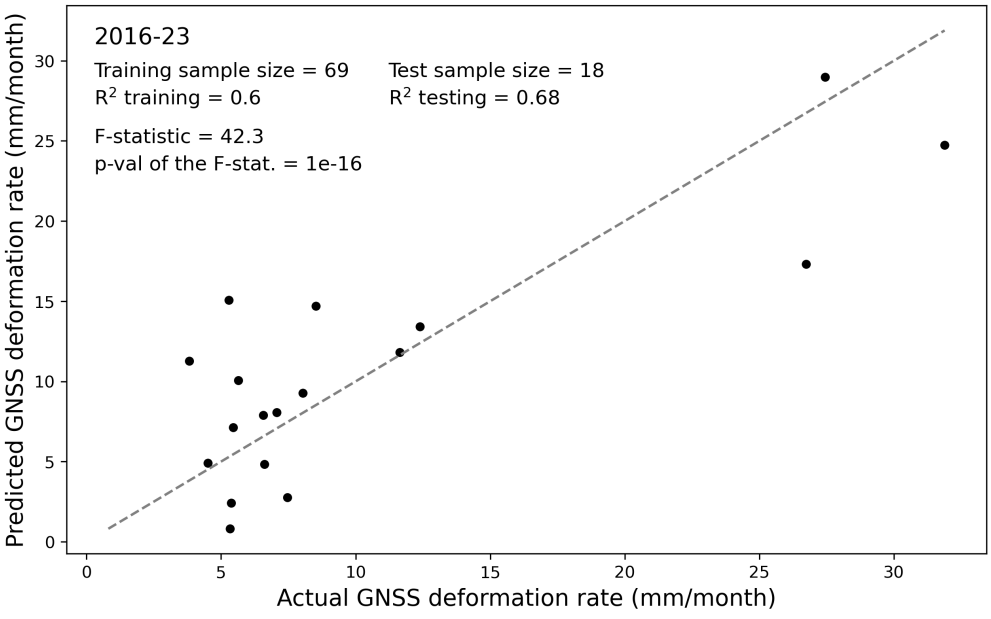

Figure B3. MLR model results from the testing data subset using the monthly-averaged air and surface temperature, AL mean temperature, and Q_G at 3.5 m depth as drivers of the GNSS deformation rate. Grey dashed line is a 1:1 line for scale. Data source: PERMOS and PermaSense.

https://doi.org/10.5194/egusphere-2025-3029
Preprint. Discussion started: 29 August 2025

Appendix C: Deformation profiles, time series and unique events

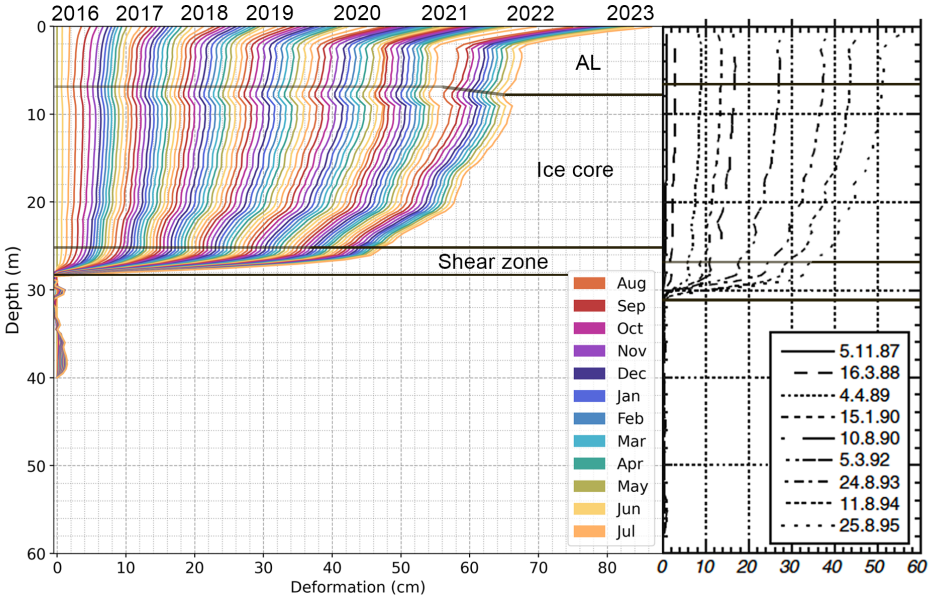

Figure C1. Monthly cumulative deformation profiles from the inclinometer data in both the 1987 and the 2015 borehole at Murtèl rock glacier. Graph of old deformation profiles adapted from Arenson et al. (2002).

https://doi.org/10.5194/egusphere-2025-3029
Preprint. Discussion started: 29 August 2025

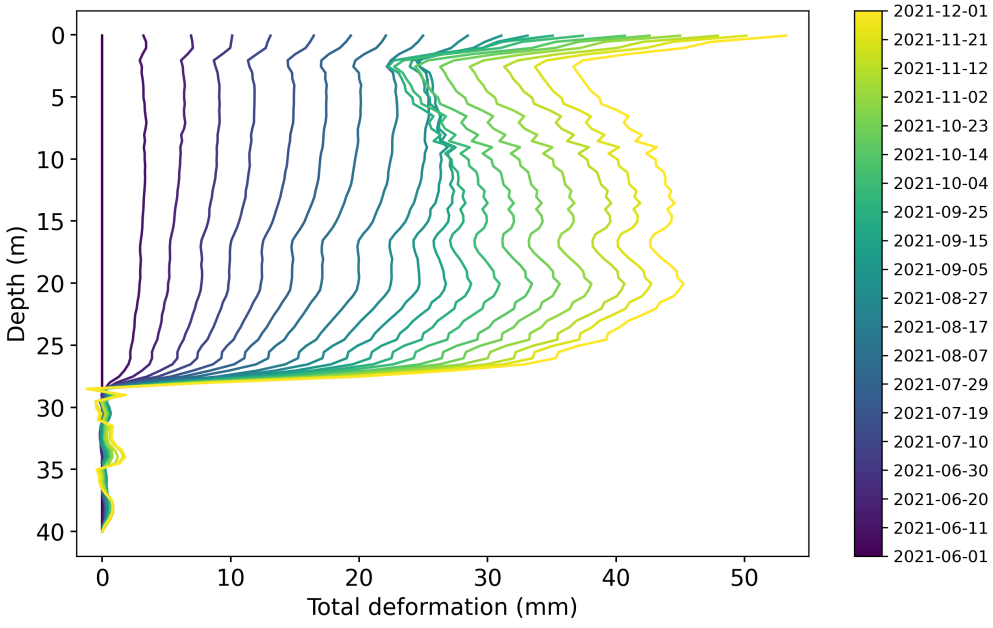

Figure C2. Vertical deformation profile from June to December 2021 during the unique deceleration event measured by the inclinometer in Murtèl 2015 borehole.

https://doi.org/10.5194/egusphere-2025-3029
Preprint. Discussion started: 29 August 2025

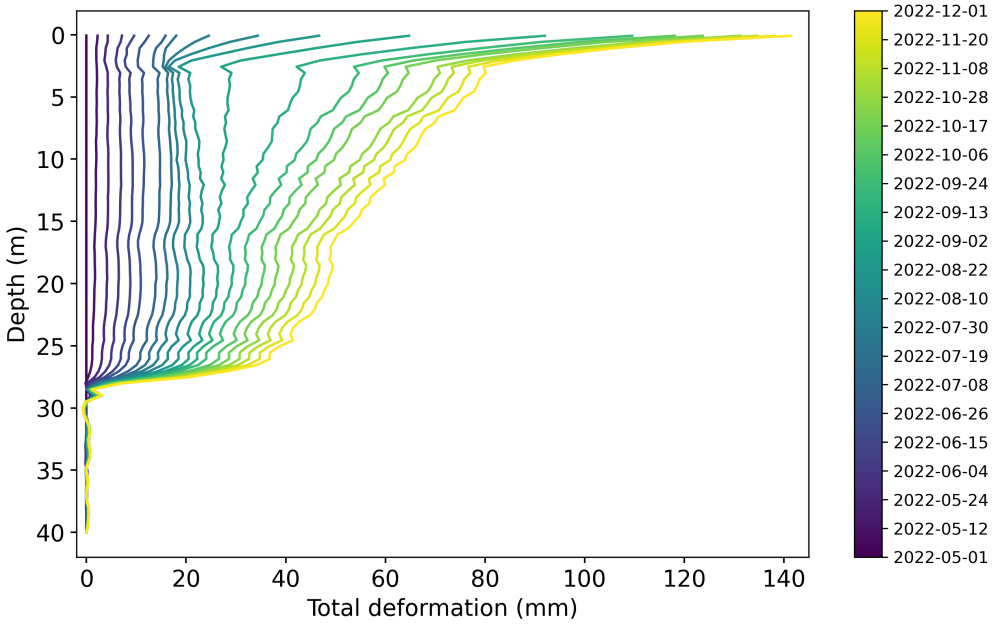

Figure C3. Vertical deformation profile from May to December 2022 during the unique deceleration event measured by the inclinometer in Murtèl 2015 borehole.

https://doi.org/10.5194/egusphere-2025-3029
Preprint. Discussion started: 29 August 2025

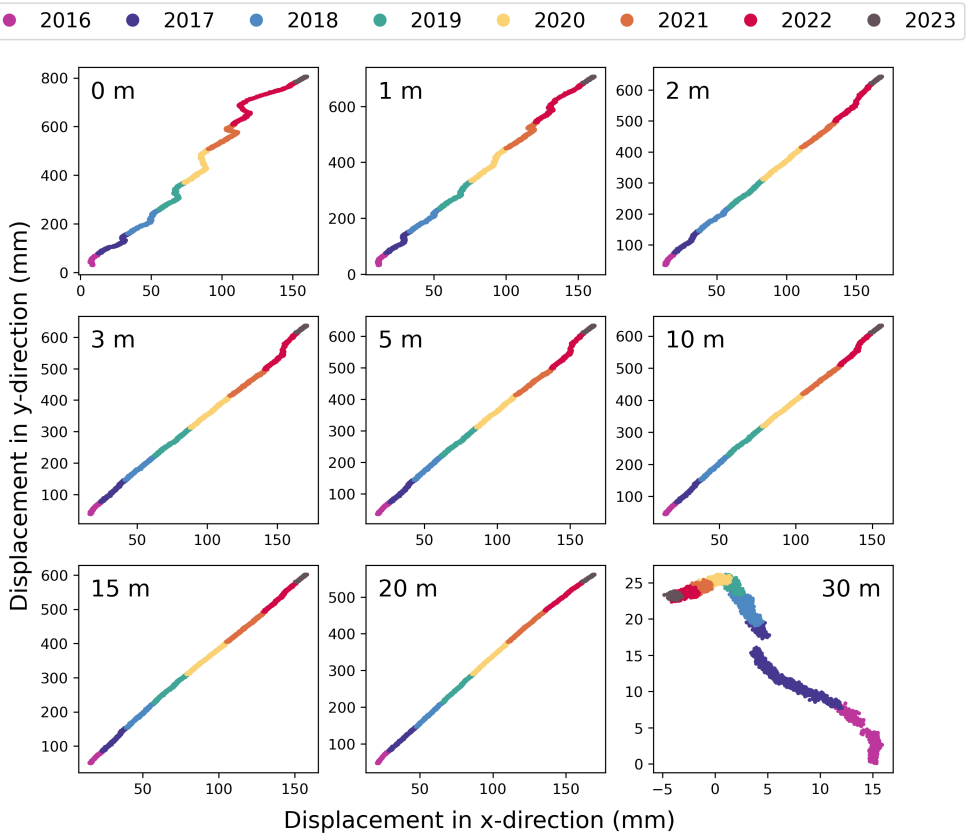

Figure C4. Top-down view of the horizontal direction of the borehole inclinometer movement where the x-direction aligns with West and y-direction with North.

https://doi.org/10.5194/egusphere-2025-3029
Preprint. Discussion started: 29 August 2025

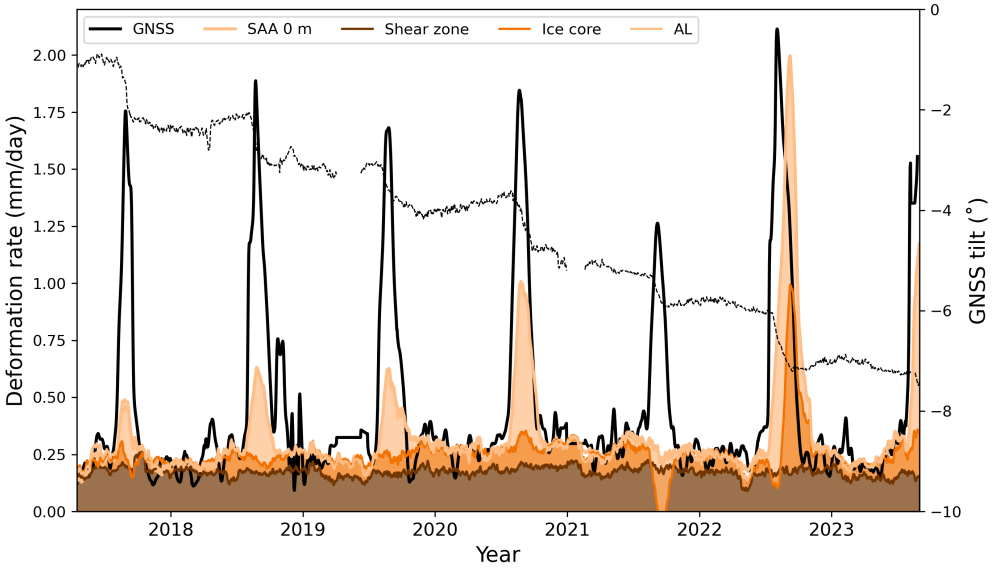

Figure C5. Daily deformation rate measured at the surface of the SAA inclinometer in the 2015 borehole and that by the GNSS station at Murtèl rock glacier. The inclination (tilt) angle measured by the GNSS station is also plotted. Data source: PERMOS and PermaSense.

Author contributions. GS performed the data preparation and analysis for this study and wrote the manuscript. IR, JB and AV provided supervision with the interpretation of the data and the editing of the manuscript. JB supplied the GNSS data and contributed to its comparison with other displacement data.

Competing interests. The authors declare that they have no conflict of interest.

Acknowledgements. The findings presented in this paper are largely based on the data produced by the new 2015 borehole drilled in Murtèl rock glacier. The drilling and maintenance of the borehole would not have been possible without the investment by PERMOS and its funding bodies, SensAlpin, and especially Alexander Bast, who organized and supervised the drilling campaign. We also acknowledge Alessandro Cicoira, Tobias Bolch and Diego Wasser for their support in maintaining measurements and the initial data viewing and handling. PERMOS also carried out the installation and operation of the on-site meteorological station at Murtèl rock glacier.

https://doi.org/10.5194/egusphere-2025-3029
Preprint. Discussion started: 29 August 2025

References

Amschwand, D., Scherler, M., Hoelzle, M., Krummenacher, B., Haberkorn, A., Kienholz, C., and Gubler, H.: Surface heat fluxes at coarse-blocky Murtèl rock glacier (Engadine, eastern Swiss Alps), https://doi.org/10.5194/egusphere-2023-2109, 2023.

Amschwand, D., Tschan, S., Scherler, M., Hoelzle, M., Krummenacher, B., Haberkorn, A., Kienholz, C., Aschwanden, L., and Gubler, H.: On the hydrological significance of rock glaciers: A case study from Murtèl rock glacier (Engadine, eastern Swiss Alps) using below-ground energy-flux measurements, ground-ice melt observations and hydrological measurements, https://doi.org/10.5194/egusphere-2024-844, 2024.

Arenson, L., Hoelzle, M., and Springman, S.: Borehole deformation measurements and internal structure of some rock glaciers in Switzerland, Permafrost and Periglacial Processes, 13, 117–135, https://doi.org/10.1002/ppp.414, 2002.

Barsch, D. and Hell, G.: Photogrammetrische Bewegungsmessungen am Blockgletscher Murtèl I, Oberengadin, Schweizer Alpen, Zeitschrift für Gletscherkunde und Glazialgeologie, 11, 111–142, 1976.

Bast, A., Kenner, R., and Phillips, M.: Short-term cooling, drying and deceleration of an ice-rich rock glacier, https://doi.org/10.5194/egusphere-2024-269, 2024.

Benedict, J. B., Benedict, R. J., and Sanville, D.: Arapaho Rock Glacier, Front Range, Colorado, U.S.A.: A 25-Year Resurvey, Arctic and Alpine Research, 18, 349–352, https://doi.org/10.1080/00040851.1986.12004096, 1986.

Buchli, T., Merz, K., Zhou, X., Kinzelbach, W., and Springman, S. M.: Characterization and Monitoring of the Furggwanghorn Rock Glacier, Turtmann Valley, Switzerland: Results from 2010 to 2012, Vadose Zone Journal, 12, 1–15, https://doi.org/10.2136/vzj2012.0067, 2013.

Buchli, T., Kos, A., Limpach, P., Merz, K., Zhou, X., and Springman, S. M.: Kinematic investigations on the Furggwanghorn Rock Glacier, Switzerland, Permafrost and Periglacial Processes, 29, 3–20, https://doi.org/10.1002/ppp.1968, 2018.

Bucki, A. K. and Echelmeyer, K. A.: The flow of Fireweed rock glacier, Alaska, U.S.A., Journal of Glaciology, 50, 76–86, https://doi.org/10.3189/172756504781830213, 2004.

Cicoira, A., Beutel, J., Faillettaz, J., Gärtner-Roer, I., and Vieli, A.: Resolving the influence of temperature forcing through heat conduction on rock glacier dynamics: a numerical modelling approach, The Cryosphere, 13, 927–942, https://doi.org/10.5194/tc-13-927-2019, 2019a.

Cicoira, A., Beutel, J., Faillettaz, J., and Vieli, A.: Water controls the seasonal rhythm of rock glacier flow, Earth and Planetary Science Letters, 528, 115 844, https://doi.org/10.1016/j.epsl.2019.115844, 2019b.

Cicoira, A., Marcer, M., Gärtner-Roer, I., Bodin, X., Arenson, L. U., and Vieli, A.: A general theory of rock glacier creep based on in-situ and remote sensing observations, Permafrost and Periglacial Processes, 32, 139–153, https://doi.org/10.1002/ppp.2090, 2021.

Cicoira, A., Weber, S., Biri, A., Buchli, B., Delaloye, R., Da Forno, R., Gärtner-Roer, I., Gruber, S., Gsell, T., Hasler, A., Lim, R., Limpach, P., Mayoraz, R., Meyer, M., Noetzli, J., Phillips, M., Pointner, E., Raetzo, H., Scapozza, C., Strozzi, T., Thiele, L., Vieli, A., Vonder Mühll, D., Wirz, V., and Beutel, J.: In situ observations of the Swiss periglacial environment using GNSS instruments, Earth System Science Data, 14, 5061–5091, https://doi.org/10.5194/essd-14-5061-2022, 2022.

Emmert, A. and Kneisel, C.: Internal structure of two alpine rock glaciers investigated by quasi-3-D electrical resistivity imaging, The Cryosphere, 11, 841–855, https://doi.org/10.5194/tc-11-841-2017, 2017.

Fey, C. and Krainer, K.: Analyses of UAV and GNSS based flow velocity variations of the rock glacier Lazaun (Ötztal Alps, South Tyrol, Italy), Geomorphology, 365, 107 261, https://doi.org/10.1016/j.geomorph.2020.107261, 2020.

https://doi.org/10.5194/egusphere-2025-3029
Preprint. Discussion started: 29 August 2025

Gärtner-Roer, I. and Hoelzle, M.: Rockglaciers of the Engadine, in: Landscapes and Landforms of Switzerland, edited by Reynard, E., pp. 235–248, Springer International Publishing, Cham, https://doi.org/10.1007/978-3-030-43203-4_16, series Title: World Geomorphological Landscapes, 2021.

Haberkorn, A., Kenner, R., Noetzli, J., and Phillips, M.: Changes in Ground Temperature and Dynamics in Mountain Permafrost in the Swiss Alps, Frontiers in Earth Science, 9, 626 686, https://doi.org/10.3389/feart.2021.626686, 2021.

Haeberli, W.: Creep of Mountain Permafrost: Internal Structure and Flow of Alpine Rock Glaciers, Ph.D. thesis, ETH Zürich, Zürich, 1985.

Haeberli, W., Huder, J., Keusen, H. R., Pika, J., and Röthlisberger, H.: CORE DRILLING THROUGH ROCK GLACIER-PERMAFROST, https://www.researchgate.net/publication/245800726, 1988.

Haeberli, W., Hoelzle, M., Kääb, A., Keller, F., Mühll, D. V., and Wagner, S.: Ten years after the drilling through the permafrost of the active rock glacier Murtel, eastern Swiss Alps : Answered questions and new perspectives, vol. 55, pp. 403–410, Collection Nordicana, Yellowknife, Canada, https://api.semanticscholar.org/CorpusID:51799942, 1998.

Haeberli, W., Hallet, B., Arenson, L., Elconin, R., Humlum, O., Kääb, A., Kaufmann, V., Ladanyi, B., Matsuoka, N., Springman, S., and Mühll, D. V.: Permafrost creep and rock glacier dynamics, Permafrost and Periglacial Processes, 17, 189–214, https://doi.org/10.1002/ppp.561, 2006.

Hoelzle, M., Wegmann, M., and Krummenacher, B.: Miniature Temperature Dataloggers for mapping and monitoring of permafrost in high mountain areas: First experience from the Swiss Alps, Permafrost and Periglacial Processes, 10, 113–124, https://doi.org/10.1002/(SICI)1099-1530(199904/06)10:23.0.CO;2-A, 1999.

Hoelzle, M., Mühll, D. V., and Haeberli, W.: Thirty years of permafrost research in the Corvatsch-Furtschellas area, Eastern Swiss Alps: A review, Norsk Geografisk Tidsskrift - Norwegian Journal of Geography, 56, 137–145, https://doi.org/10.1080/00291950276005646 8, 2002.

Ikeda, A., Matsuoka, N., and Kääb, A.: Fast deformation of perennially frozen debris in a warm rock glacier in the Swiss Alps: An effect of liquid water, Journal of Geophysical Research: Earth Surface, 113, 2007JF000 859, https://doi.org/10.1029/2007JF000859, 2008.

Keller, F.: Interaktionen zwischen Schnee und Permalrost: eine Grundlagenstudie im Oberengadin., Tech. Rep. 127, Versuchsanstalt für Wasserbau, Hydrologie und Glaziologie, ETH Zürich, 1994.

Kellerer-Pirklbauer, A., Bodin, X., Delaloye, R., Lambiel, C., Gärtner-Roer, I., Bonnefoy-Demongeot, M., Carturan, L., Damm, B., Eulenstein, J., Fischer, A., Hartl, L., Ikeda, A., Kaufmann, V., Krainer, K., Matsuoka, N., Morra Di Cella, U., Noetzli, J., Seppi, R., Scapozza, C., Schoeneich, P., Stocker-Waldhuber, M., Thibert, E., and Zumiani, M.: Acceleration and interannual variability of creep rates in mountain permafrost landforms (rock glacier velocities) in the European Alps in 1995–2022, Environmental Research Letters, 19, 034 022, https://doi.org/10.1088/1748-9326/ad25a4, 2024.

Kenner, R., Pruessner, L., Beutel, J., Limpach, P., and Phillips, M.: How rock glacier hydrology, deformation velocities and ground temperatures interact: Examples from the Swiss Alps, Permafrost and Periglacial Processes, 31, 3–14, https://doi.org/10.1002/ppp.2023, 2020.

Krainer, K. and Mostler, W.: Hydrology of Active Rock Glaciers: Examples from the Austrian Alps, Arctic, Antarctic, and Alpine Research, 34, 142–149, https://doi.org/10.1080/15230430.2002.12003478, 2002.

Kääb, A., Frauenfelder, R., and Roer, I.: On the response of rockglacier creep to surface temperature increase, Global and Planetary Change, 56, 172–187, https://doi.org/10.1016/j.gloplacha.2006.07.005, 2007.

Ladanyi, B.: Rheology of ice/rock systems and interfaces, Permafrost, 1-2, 621–626, https://www.arlis.org/docs/vol1/ICOP/55700698/Pdf/Chapter_110.pdf, 2003.

https://doi.org/10.5194/egusphere-2025-3029
Preprint. Discussion started: 29 August 2025

Lambiel, C. and Delaloye, R.: Contribution of real-time kinematic GPS in the study of creeping mountain permafrost: examples from the Western Swiss Alps, Permafrost and Periglacial Processes, 15, 229–241, https://doi.org/10.1002/ppp.496, 2004.

Lugon, R. and Stoffel, M.: Rock-glacier dynamics and magnitude–frequency relations of debris flows in a high-elevation watershed: Ritigraben, Swiss Alps, Global and Planetary Change, 73, 202–210, https://doi.org/10.1016/j.gloplacha.2010.06.004, 2010.

Mittaz, C., Hoelzle, M., and Haeberli, W.: First results and interpretation of energy-flux measurements over Alpine permafrost, Annals of Glaciology, 31, 275–280, https://doi.org/10.3189/172756400781820363, 2000.

Moore, P. L.: Deformation of debris-ice mixtures: DEFORMATION OF DEBRIS-ICE MIXTURES, Reviews of Geophysics, 52, 435–467, https://doi.org/10.1002/2014RG000453, 2014.

Noetzli, J., Arenson, L. U., Bast, A., Beutel, J., Delaloye, R., Farinotti, D., Gruber, S., Gubler, H., Haeberli, W., Hasler, A., Hauck, C., Hiller, M., Hoelzle, M., Lambiel, C., Pellet, C., Springman, S. M., Vonder Muehll, D., and Phillips, M.: Best Practice for Measuring Permafrost Temperature in Boreholes Based on the Experience in the Swiss Alps, Frontiers in Earth Science, 9, 607 875, https://doi.org/10.3389/feart.2021.607875, 2021.

Noetzli, J., Isaksen, K., Barnett, J., Christiansen, H. H., Delaloye, R., Etzelmüller, B., Farinotti, D., Gallemann, T., Guglielmin, M., Hauck, C., Hilbich, C., Hoelzle, M., Lambiel, C., Magnin, F., Oliva, M., Paro, L., Pogliotti, P., Riedl, C., Schoeneich, P., Valt, M., Vieli, A., and Phillips, M.: Enhanced warming of European mountain permafrost in the early 21st century, Nature Communications, 15, 10 508, https://doi.org/10.1038/s41467-024-54831-9, 2024.

Nye, J. F.: The Mechanics of Glacier Flow, Journal of Glaciology, 2, 82–93, https://doi.org/10.3189/S0022143000033967, 1952.

PERMOS: Swiss Permafrost Bulletin 2023, Tech. Rep. 5, Swiss Permafrost Monitoring Network PERMOS, 2024.

RGIK: Rock Glacier Velocity as an associated parameter of ECV Permafrost: Baseline concepts (Version 3.2), https://bigweb.unifr.ch/Science/Geosciences/Geomorphology/Pub/Website/IPA/CurrentVersion/Current_RockGlacierVelocity.pdf, 2023.

Roer, I.: Rockglacier Kinematics in a High Mountain Geosystem, Ph.D. thesis, Universität Bonn, https://hdl.handle.net/20.500.11811/10497, 2007.

Roer, I., Kääb, A., and Dikau, R.: Rockglacier acceleration in the Turtmann valley (Swiss Alps): Probable controls, Norsk Geografisk Tidsskrift - Norwegian Journal of Geography, 59, 157–163, https://doi.org/10.1080/00291950510020655, 2005.

Scherler, M., Schneider, S., Hoelzle, M., and Hauck, C.: A two-sided approach to estimate heat transfer processes within the active layer of the Murtèl–Corvatsch rock glacier, Earth Surface Dynamics, 2, 141–154, https://doi.org/10.5194/esurf-2-141-2014, 2014.

Schneider, S., Hoelzle, M., and Hauck, C.: Influence of surface and subsurface heterogeneity on observed borehole temperatures at a mountain permafrost site in the Upper Engadine, Swiss Alps, The Cryosphere, 6, 517–531, https://doi.org/10.5194/tc-6-517-2012, 2012.

SwissTopo: https://www.swisstopo.admin.ch/de, 2025.

Vonder Mühll, D. and Haeberli, W.: Thermal Characteristics of the Permafrost within an Active Rock Glacier (Murtèl/Corvatsch, Grisons, Swiss Alps), Journal of Glaciology, 36, 151–158, https://doi.org/10.3189/S0022143000009382, 1990.

Vonder Mühll, D., Stucki, T., and Haeberli, W.: BOREHOLE TEMPERATURES IN ALPINE PERMAFROST: A TEN YEAR SERIES., vol. 55, pp. 1089–1095, Collection Nordicana, Yellowknife, Canada, https://www.arlis.org/docs/vol1/ICOP/40770716/CD-ROM/Proceedings/PDF001189/164016.pdf, 1998.

Wahrhaftig, C. and Cox, A.: ROCK GLACIERS IN THE ALASKA RANGE, Geological Society of America Bulletin, 70, 383, https://doi.org/10.1130/0016-7606(1959)70[383:RGITAR]2.0.CO;2, 1959.

https://doi.org/10.5194/egusphere-2025-3029
Preprint. Discussion started: 29 August 2025

Wirz, V., Beutel, J., Gruber, S., Gubler, S., and Purves, R. S.: Estimating velocity from noisy GPS data for investigating the temporal variability of slope movements, Natural Hazards and Earth System Sciences, 14, 2503–2520, https://doi.org/10.5194/nhess-14-2503-2014, 2014.

Wirz, V., Gruber, S., Purves, R. S., Beutel, J., Gärtner-Roer, I., Gubler, S., and Vieli, A.: Short-term velocity variations at three rock glaciers and their relationship with meteorological conditions, Earth Surface Dynamics, 4, 103–123, https://doi.org/10.5194/esurf-4-103-2016, 2016.